JBAAR
Journal of Basic and Applied Research in Biomedicine
ISSN 2413-7014

Original Article

Computed Tomography–Based Quantitative Morphometry Reveals Distinct Airway Remodelling in COVID-19 versus Community-Acquired Pneumonia

Gihad Ibrahim

Faculty of Engineering, Mashreq University, Khartoum North, Khartoum, Sudan

*Corresponding Author: gibrahim@mashreq.edu.sd

Received: 01-08-2025
Revised: 16-08-2025
Published: 26-08-2025

Keywords:
COVID-19, Airway remodelling, Computed tomography, Bronchial geometry, Pneumonia

Abstract: ***Purpose***: To quantitatively characterize airway structural changes in COVID-19 and compare them to those observed in community-acquired pneumonia (CAP), using computed tomography (CT)-based Morphometry. The study aims to evaluate whether COVID-19 and CAP produce distinct patterns of airway remodelling across multiple geometric metrics. ***Materials and methods:*** High-resolution chest CT scans from 80 COVID-19 patients (stratified into low- and high-severity subgroups), 38 CAP patients, and 28 healthy controls were analysed. Airway parameters—hydraulic diameter (Dh (mm)), hydraulic ratio (Xh), airway circularity (Cr), and airway thickness (TA (mm))—were measured across the first 5–6 bronchial generations using 3D reconstruction and geodesic labelling. Statistical comparisons employed Kruskal–Wallis and regression analyses. ***Results***: COVID-19 exhibited proximal airway enlargement but distal narrowing, contrasting with CAP's uniform reduction in airway efficiency ($p < 0.01$). Xh gradients revealed compensatory adaptation in COVID-19's major airways (steeper slope in severe cases, $p = 0.013$) but significant distal dysfunction (−12% Xh vs. CAP, $p < 0.001$). Circularity showed focal geometric distortion in COVID-19 versus CAP's homogeneous expansion ($p < 0.001$). TA (mm) analysis identified diffuse thinning in COVID-19 (vs. CAP's mild thickening, $p = 0.189$), with superimposed focal thromboinflammatory thickenings. ***Conclusions***: COVID-19 and CAP induce fundamentally different patterns of airway remodelling. COVID-19 is associated with proximal airway dilation and disrupted distal tapering, whereas CAP results in uniform narrowing. These morphometric profiles may contribute to differences in airflow limitation and ventilation–perfusion mismatch, which could inform disease-specific monitoring, prognostication, and selection of therapeutic strategies. Future research should explore the relationship between these structural signatures and clinical outcomes, including recovery trajectory and long-term pulmonary function.

Cite this article as: Ibrahim, G. (2025). Computed Tomography–Based Quantitative Morphometry Reveals Distinct Airway Remodelling in COVID-19 versus Community-Acquired Pneumonia. Journal of Basic and Applied Research in Biomedicine, 11(1): 30-37

INTRODUCTION

Respiratory diseases are usually characterized by structural and functional alterations in the airways morphology, which significantly impact pulmonary mechanics and gas exchange. While traditionally viewed as a pulmonary disorder, Coronavirus disease 2019 (COVID-19) has increasingly been recognized as a multisystem disease with predominant cardiovascular manifestations, including endothelial injury, microthrombosis, and systemic inflammation (Bansal, 2020; Louis et al., 2023), rather than a purely respiratory condition. However, its profound effects on the lungs, such as silent hypoxemia and heterogeneous radiographic findings, highlight the need to investigate airway-specific pathology (D'Arena et al., 2021; Swenson et al., 2021). In contrast, community-acquired pneumonia (CAP) primarily involves direct inflammatory damage to the lung parenchyma and airways due to bacterial or viral pathogens (Long et al., 2022). Despite extensive research on parenchymal changes in COVID-19 (e.g., ground-glass opacities (Cozzi et al., 2021; Roig-Marín, 2024)), systematic comparisons of central airway geometry between COVID-19 and CAP remain limited. Understanding these differences is critical, as airway remodelling may underlie distinct clinical presentations, such as the dissociation between severe hypoxemia and relatively preserved lung compliance in COVID-19 (Swenson et al., 2021).

Quantitative assessment of airway geometry through high-resolution computed tomography (CT) and advanced 3D reconstruction techniques has emerged as a powerful tool for characterizing pulmonary pathology (Dournes, 2025; Mahdavi et al., 2023). Precise morphometric analysis of key parameters, including hydraulic diameter (Dh (mm)), hydraulic ratio (Xh), airway circularity (Cr), and airway thickness (TA (mm)), provides critical insights into airflow dynamics and disease mechanisms (Choi et al., 2017). For instance, Dh (mm) reflects luminal narrowing and flow resistance, while Xh captures the efficiency of proximal-to-distal tapering, a hallmark of normal bronchial structure. Similarly, Cr quantifies geometric distortions in airway cross-sections, and TA (mm) differentiates inflammatory thickening from atrophic remodelling (Eskandari et al., 2015; Goodwill et al., 2017; Ortiz-Puerta et al., 2023). Studies in other respiratory diseases, such as asthma and chronic obstructive pulmonary disease (COPD), have demonstrated the clinical relevance of such measurements in predicting disease severity and therapeutic response (Choi et al., 2017; Ortiz-Puerta et al., 2023; Park et al., 2019). By applying these well-established morphometric techniques to COVID-19 and CAP, this study bridges a critical gap in understanding how distinct pathogenic mechanisms, vascular injury in COVID-19 versus direct microbial damage in CAP, manifest in airway architecture and function.

Previous CT-based studies have demonstrated that bacterial pneumonia frequently presents with homogeneous parenchymal consolidation and smooth, often uniform changes in airway wall thickness and lumen size (Long et al., 2022; Mahdavi et al., 2023). Such uniform narrowing patterns are thought to contribute to airflow resistance and ventilation-perfusion mismatch during the acute infectious phase (Aghasafari et al., 2019). While these findings are well established for bacterial infections, the ability to quantitatively describe such changes using 3D morphometric metrics like Dh, Xh, and Cr has been limited.

In contrast, structural airway changes in COVID-19 are less well defined and appear to follow a different morphologic trajectory (Dhochak et al., 2020; Patil et al., 2023; Shi et al., 2020). For instance, Swenson et al. (2021) and D'Arena et al. (2021)

reported that severe COVID-19 cases are associated with unexpected radiologic findings such as central airway enlargement, likely reflecting regional overdistension or compensatory airflow redistribution. Such dilation is not typical of CAP and may relate to the unique vascular and alveolar pathophysiology in COVID-19. Studies also have identified mucin abnormalities (MUC5AC/MUC5B) in COVID-19 airways, implicating mucus plugging in airflow obstruction (Meyerholz & Reznikov, 2022), while CAP typically exhibits diffuse inflammatory narrowing. These observations are supported by recent morphometric studies (e.g., Roig-Marín, 2024) describing variable bronchial wall geometry and luminal irregularity, although these reports often lack quantitative segmentation by airway generation or lobar distribution.

This study provides a comprehensive analysis of airway remodelling patterns distinguishing COVID-19 from community-acquired pneumonia through quantitative CT morphometry. These morphometric differences correlate with disease severity and offer structural insights into COVID-19's unique clinical presentation, particularly the dissociation between hypoxemia and lung compliance. The identification of distinct remodelling patterns establishes airway architecture as an important pathological domain in COVID-19, with potential implications for both acute respiratory management and long-term pulmonary monitoring

MATERIALS AND METHOD

Ethical Approval

The CT scans utilized in this study were obtained from the publicly available COVID-19 –CT-MD dataset (Afshar et al., 2021). The original study was conducted in accordance with ethical standards guidelines under Certification No. 30013394 (Concordia University, Montreal, Canada), which approves the secondary use of medical data, and written informed consent was obtained from all participants by the primary investigators. The secondary use of this dataset for the present analysis was approved by the Mashreq University Institutional Review Board.

Study Population

146 CT scans of the human's thorax are utilized in this study. The images were classified into three main groups: (1) the COVID-19 group, which contains 80 subjects of positive COVID-19 pneumonia patients that were confirmed by Polymerase Chain Reaction (PCR) testing. Group (2), the CAP group, includes 38 subjects diagnosed with Community Acquired Pneumonia and confirmed negative for COVID-19 via PCR testing. Group (3) contains CT-scans of 28 healthy and non-smoking subjects with no history of pulmonary diseases. The COVID-19 group was further divided into two subgroups, the low severity (LCVD) and the high severity (HCVD), based on the COVID-19 phenotype as explained in Gattinoni et al. (2020). The classification was based on the cumulative voxels distribution of the CT-scan. Patients with >50% of lung voxels exceeding −300 HU (indicating consolidation) were classified as HCVD, consistent with Gattinoni's Type H phenotype. LCVD cases showed <30% involvement in −750 to −300 HU ranges. The LCVD subgroup contained 42 subjects and the HCVD subgroup contained 38 subjects. The selection of the subjects were based on three main criteria, (1) no pulmonary disease history other than COVID-19 and/or CAP, (2) no airway or esophageal intubation, and (3) CT-scan clarity sufficient to construct up to the 6th generation of the bronchial tree with minimum or no manual editing.

CT Acquisition Parameters

CT scans generate detailed 3D anatomical representations through sequential 2D cross-sectional images (slices). The COVID-19 –CT-MD dataset scans were acquired using a SIEMENS SOMATOM Scope scanner in axial view with helical acquisition. Images were reconstructed via Filtered Back Projection (FBP) with a 512×512 matrix and D40s kernel to optimize spatial resolution while minimizing noise. All datasets were stored in Digital Imaging and Communications in Medicine (DICOM) format with Hounsfield Unit calibration. The scanning parameters along with other clinical data statistics of the various groups are listed in Table 1. Slice thickness, Peak Kilovoltage (kVP), and exposure time are almost the same with a few variations in a few CAP cases. Distance of Source to detector and Distance of Source to patient, which are traditionally referred to as SID and SOD, respectively, are also the same in all cases except for a few CAP cases (Afshar et al., 2021).

Airway Segmentation and Labelling

The CT-images were imported to the medical image processing software Materialize Mimics (v21.0, Materialise NV, Leuven, Belgium) for segmentation and 3D reconstruction of the bronchial tree of each subject. All the generated 3D models were visually inspected by an expert and manually edited when necessary to cover up to the 6th generation of the bronchial tree. A centreline was eventually generated for each model, which will be used for computing the anatomical structural variables. The airway branches were labelled in accordance to the geodesic atlas-based labelling method of Feragen et al. (2015) as shown in Figure 1. An additional bifurcation (not included in the atlas) was added to the middle lobe branch R6 and its branches were labelled as R11 and R12.

Table 1 Scanning parameters and clinical data of the examined subject groups.

CT-Scan Parameter	COVID-19		CAP	Normal
	LCVD	HCVD		
Slice Thickness (mm)	2	2	2	2
Peak Kilovoltage (kVp)	110-130	110-130	110-120	110
X-ray Tube Current (mA)	153-343	153-343	94-500	132-343
SID (mm)	940	940	940-1040	940
SOD (mm)	535	535	535-570	535
Exposure values (mAs)	61.2-180.0	61.2-180.0	38.4-175.24	60.4-163.71
Clinical Data				
Subjects, n	42	38	38	28
Age, yr	50.0±17.0	50.5±19.5	45.5±24.5	43.0±25.0
Gender, female (%)	28.2	35.3	47.3	35
Weigh (Kg).	50±32.5	81±16	84±34	81±29

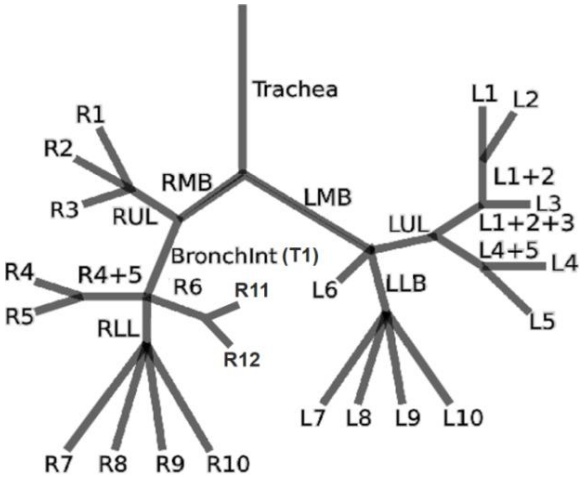

Figure 1: Airway branch labelling schematic following the geodesic atlas-based system (Feragen et al., 2015). Branches R11 and R12 labels are not included in the atlas.

Morphometric Analysis Variables

To analyse the effect of COVID-19 on the anatomical structure of the bronchial tree, four local structural variables were extracted from the 3D models of the examined subjects.

(1) The hydraulic diameter(Dh): This is a significant parameter of the pulmonary flow resistance indicating luminal narrowing. Dh (mm) was calculated as: (Choi et al., 2015)

$$Dh = \frac{4 \times LA}{P_e} \quad (1)$$

Where P_e (mm) is the perimeter of the luminal area and LA (mm^2) is the luminal cross sectional area.

(2) The hydraulic ratio (Xh): This parameter is a non-dimensional number represents a dimensionless parameter that quantifies the efficiency of airflow through bronchial segments by characterizing the relationship between a cross-section's hydraulic diameter and its subscribing diameter. Mathematically, Xh is calculated as:

$$Xh = \frac{Dh}{Ds} \quad (2)$$

Where Dh (mm) is the hydraulic diameter and Ds (mm) is the subscribing diameter of the airway segment.
This ratio essentially normalizes the effective luminal diameter against its theoretical maximum, providing a standardized measure of flow efficiency independent of absolute airway size.

(3) The airway circularity Cr: This non-dimensional number is an indication of the heterogeneous airway luminal shape and it was calculated as

$$Cr = \frac{\pi D_{ave}}{P_e} \quad (3)$$

where D_{ave} (mm) is the average luminal diameter, and P_e (mm) is the perimeter of the luminal area.

D_{ave} was calculated as (Choi et al., 2015)

$$D_{ave} = \sqrt{4 \times LA/\pi} \quad (4)$$

Where LA (mm^2) is the luminal cross sectional area.

If $Cr = 1$, this indicates that the luminal cross sectional area has a perfect circular shape, and it decreases negatively as the non-circularity of luminal cross sectional increases.

(4) Airway thickness (TA): This parameter represents the volumetric distance metric between opposing surfaces of the segmented airway model, reflecting the overall lumen-to-lumen distance (in mm) across the bronchial structure. This is a triangular based analysis in the 3D space, where TA (mm) is considered as the distance between one triangular surface of the airway model and the opposite shear one. In general, this analysis can give a good indication of airway volume distortion.
Statistical analysis was performed using IBM SPSS Statistics (Version 28.0, IBM Corp., Armonk, NY, USA). Continuous variables were expressed as mean ± standard deviation (SD) or median (interquartile range, IQR) based on distribution normality, assessed by Shapiro-Wilk tests. Group comparisons for morphometric parameters (Dh, Xh, Cr, and TA) were conducted using Kruskal–Wallis tests with post-hoc Dunn-Bonferroni corrections for non-parametric data. A two-tailed p-value <0.05 was considered statistically significant.

RESULTS

The Hydraulic Diameter

The analysis of the Dh average (mm) of the studied groups in comparison to the normal group indicates that Dh (mm), in general, increased with COVID-19 severity as shown in Figure 2. HCVD subjects exhibiting the largest airway hydraulic diameters, while CAP subjects showed a trend toward decreased or minimally altered Dh (mm) compared to Normal subjects. However, this effect was not uniform across all regions of the lung as shown in Figure 3. These observations were further backed by the Kruskal–Wallis tests that were conducted to assess the statistical differences in Dh (mm) between the examined subject-groups across airway branches. Certain branches, particularly in the upper lobes and major airways (Trachea, RMB, LMB, and T1), showed significant enlargement in COVID-19 subjects (p = 0.002), whereas some branches, including L1+2+3, R8, and R9, exhibited no significant dilation or even slight reductions. In contrast, CAP was associated with either a reduction or minimal change in Dh (mm), suggesting distinct structural effects compared to COVID-19. Distal branches such as R11, L2, and L5 experienced a significant reduction of Dh (mm) (more than 10%) in the case of LCVD exceeding that of CAP subjects, whereas the reduction of Dh (mm) at these branches in the HCVD group is negligible. In addition, direct comparisons between LCVD and HCVD groups showed significant Dh (mm) differences in multiple branches, particularly large airways and upper lobe branches, but not uniformly across all regions.

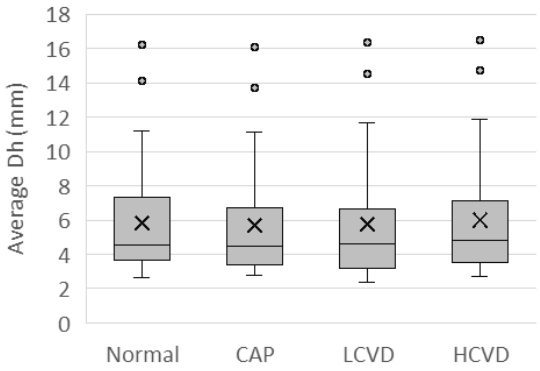

Figure 2: Comparison of average airway hydraulic diameter (Dh (mm)) across Normal, community-acquired pneumonia (CAP), low-severity COVID-19 (LCVD), and high-severity COVID-19 (HCVD) groups. Error bars indicate standard deviation.

Analysis of lobar and regional effects highlights the heterogeneous pattern of Dh (mm) alterations. For example, while R1 and R2 of the Right Upper Lobe (RUL) showed significant Dh (mm) enlargement in HCVD subjects, R3 exhibited more moderate changes. The L1+2+3 branch in the Left Upper Lobe (LUL) did not show significant Dh (mm) increases, indicating that COVID-19 does not uniformly affect all upper lobe airways. Dh (mm) alterations were less pronounced in the Right Lower Lobe (RLL) and Left Lower Lobes (LLL) regions. For example, R8 and R9 of the Right Lower Lobe did not exhibit significant change in LCVD or HCVD subjects (P = 0.289), whereas, L7, L8, and L10 of the Left Lower Lobe showed mild to moderate increase in Dh (mm) (P = 0.036).

The Hydraulic ratio (Xh)

A systematic evaluation of the Xh patterns across airway generations was performed using linear regression analysis, with branches ordered anatomically from proximal to distal and analysed separately for each lung as shown in Figure 4. This approach revealed distinct disease-specific alterations in the spatial distribution of airway flow efficiency.

In the right lung, the Normal group exhibited the steepest Xh gradient (slope = 0.0092, R^2 = 0.28), consistent with a structured proximal-to-distal tapering of hydraulic geometry. CAP patients, in contrast, showed a markedly flattened slope (0.0018) despite a similar R^2 value (0.28), suggesting that Xh remained relatively uniform throughout the right-sided airway branches in this group. Both LCVD (slope = 0.0068, R^2 = 0.19) and HCVD (slope = 0.0072, R^2 = 0.26) exhibited intermediate gradients—less steep than normal but clearly more organized than CAP. Notably, HCVD preserved a higher slope and stronger correlation compared to LCVD.

In the left lung, although the Normal group retained the same slope magnitude (0.0092), the R^2 value was substantially lower (0.099), implying greater anatomical variability or segmentation noise. The CAP group again demonstrated a flattened gradient (slope = 0.0027) with moderate fit (R^2 = 0.28), mirroring the right lung pattern. For LCVD (slope = 0.0022, R^2 = 0.044) and HCVD (slope = 0.0072, R^2 = 0.0652), regression fits were poor, particularly in LCVD.

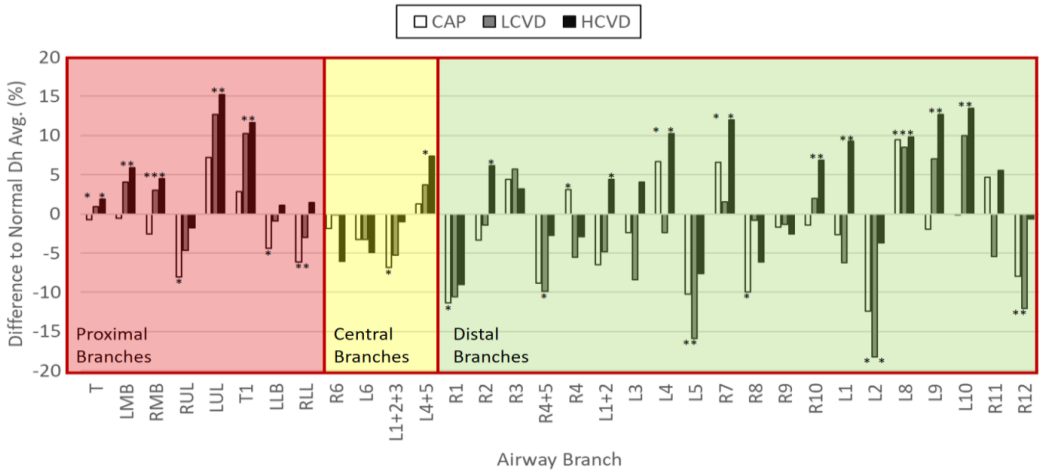

Figure 3. Difference in average hydraulic diameter (Dh, mm) relative to Normal subjects for each airway branch, comparing community-acquired pneumonia (CAP), low-severity COVID-19 (LCVD), and high-severity COVID-19 (HCVD) groups. Airway branches are organized according to the geodesic atlas–based labelling system from proximal to distal. Positive values indicate airway dilation, while negative values indicate narrowing compared to the Normal reference. * branches with Kruskal–Wallis significance $p < 0.005$.

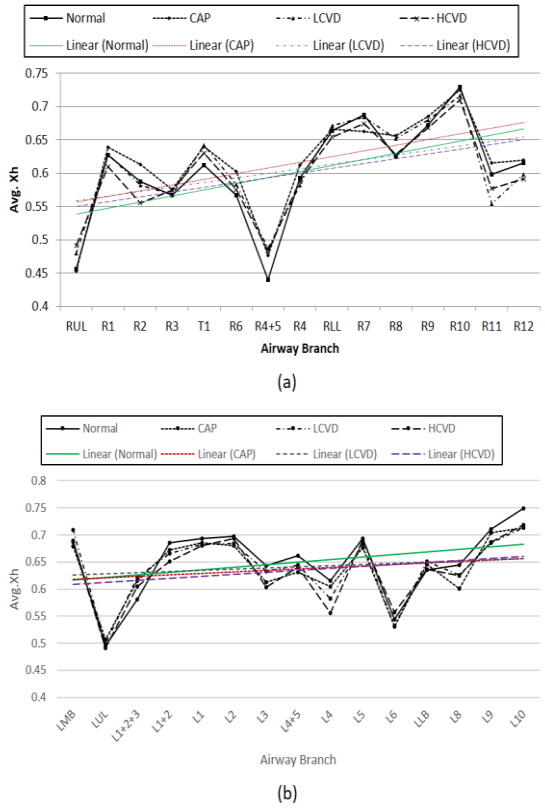

Figure 4: Linear regression slopes of hydraulic ratio (Xh) plotted against airway branch generation for (a) right lung and (b) left lung in Normal, community-acquired pneumonia (CAP), low-severity COVID-19 (LCVD), and high-severity COVID-19 (HCVD) groups. Slopes represent the rate of change in Xh from proximal to distal airways, where more negative values indicate greater tapering loss.

Airway Circularity (Cr)

The Kruskal-Wallis test revealed significant differences in Cr among the study groups ($H=42.7$, $p<0.001$) as shown in Figure 5, with post-hoc analysis demonstrating distinct patterns of luminal deformation in COVID-19 compared to both CAP and normal subjects. Normal airways maintained consistently high Cr values (median 0.892, IQR 0.831-0.923), while both disease groups showed marked reductions (CAP: median 0.768, IQR 0.679-0.812; COVID-19: median 0.747, IQR 0.653-0.798; $p<0.001$ for both comparisons).

The spatial distribution of Cr alterations differed significantly between conditions (Kruskal–Wallis $H=38.2$ for regional variation, $p<0.001$). COVID-19 patients exhibited severe proximal airway distortion, with the trachea showing significantly lower Cr than both CAP (0.493 vs. 0.814, $p=0.002$) and normal groups ($p<0.001$). Middle-generation airways in COVID-19 demonstrated relative preservation of circularity (R6: 0.708 vs. CAP 0.697, $p=0.038$), while distal airways showed greater deformation than CAP in specific segments (L8: 0.626 vs. 0.724, $p<0.001$).

Disease severity significantly influenced Cr patterns in COVID-19 ($H=25.6$ for severity stratification, $p<0.001$). HCVD patients had more pronounced Cr reduction than LCVD in upper lobes (median 0.681 vs. 0.713, $p=0.003$) and lower lobes (0.654 vs. 0.722, $p<0.001$), but showed less distortion in middle lobe segments (0.735 vs. 0.698, $p=0.021$). CAP patients displayed uniformly reduced Cr across all generations ($H=7.2$ for regional variation, $p=0.201$), with the most significant deviation from normal in distal airways (R10: 0.593 vs. normal 0.729, $p<0.001$).

Airway Thickness (TA)

The integrated analysis of TA (mm) metrics revealed distinct structural remodelling patterns across study groups, with particularly notable differences emerging between COVID-19 patients and those with community-acquired pneumonia (CAP). Although the Kruskal–Wallis test demonstrated no significant variation in median TA values ($p=0.189$), the post-hoc analysis showed a progressive increase from normal controls (5.13) in CAP to (5.25) and a reduction in COVID-19 subgroups (LCVD: 5.1; HCVD: 4.75) as shown in Figure 6(a). In addition, the dispersion analysis of the TA (mm) data through interquartile ranges (IQR) showed no significant group differences ($p=0.62$), with all cohorts displaying almost similar variability in airway thickness as shown in Figure 6(b). All groups TA (mm) data exhibited positive skewness (Normal: 0.279, CAP: 0.231, LCVD: 0.266, HCVD: 0.284). Furthermore, the Kurtosis assessment via RMS-to-mean ratios (Normal: 1.217, CAP: 1.186, LCVD: 1.163, HCVD: 1.207; $p=0.39$) provided further evidence of distinct remodelling patterns as shown in Figure 6(c).

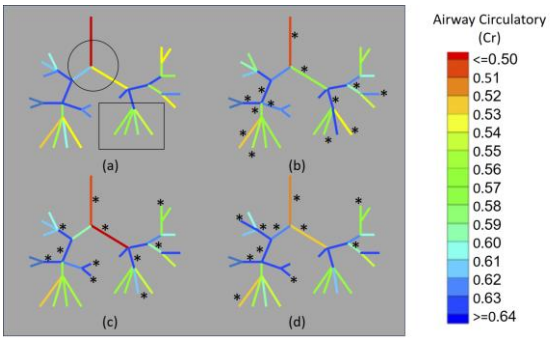

Figure 5: Schematic bronchial tree color-coded by average branch circularity (Cr). (a) Normal Group, (b) CAP Group, (c) LCVD group, and (d) HCVD group. Significant differenced observed at proximal airways (circle), and distal airways (square), while central airways circularity remodelling was minor. * branches with Kruskal-Wallis significance $p < 0.005$.

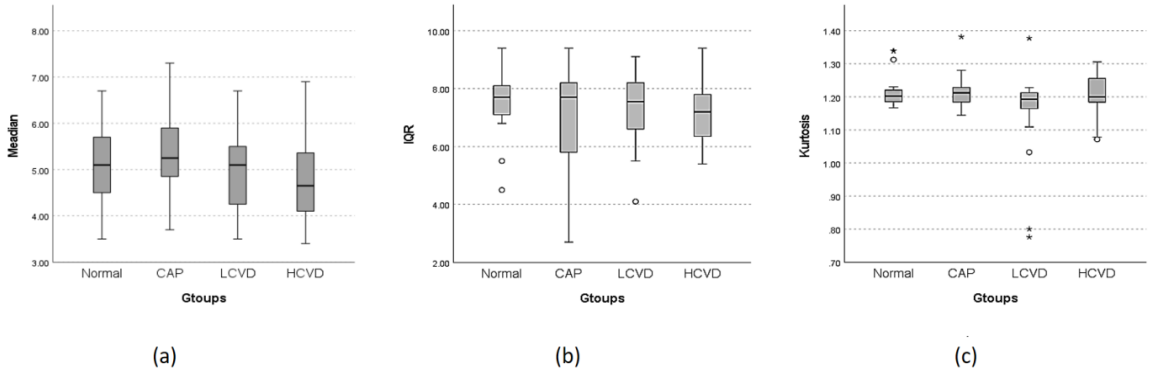

(a) (b) (c)

Figure 6: Kruskal–Wallis test of airway thickening (TA (mm)) triangular data. (a) Median, (b) IQR, and (c) Kurtosis Proxy

DISCUSSION

The findings of this study provide a detailed morphometric characterization of bronchial airway alterations in COVID-19 pneumonia compared to community-acquired pneumonia (CAP) and healthy controls. The analyses revealed distinct patterns of airway remodelling associated with COVID-19, marked by heterogeneous changes in Dh (mm), Xh, Cr, and TA (mm). These structural changes suggest unique pathophysiological mechanisms in COVID-19 that differ from those observed in CAP, potentially contributing to the distinct clinical manifestations of the disease.

One of the key observations was the significant enlargement of hydraulic diameter (Dh (mm)) in COVID-19 patients, particularly in those with high disease severity (HCVD). This dilation was most pronounced in proximal airways, such as the trachea and main bronchi, while distal branches exhibited more variable responses, including constriction in some segments. This observation is consistent with the CT-based morphometric findings of Zaremba et al. (2024), who reported bronchial enlargement of the main conducting airways in post-COVID patients. In contrast, CAP was associated with either minimal changes or slight reductions in Dh (mm), indicating a fundamentally different pattern of airway involvement, a pattern that is also consistent with earlier CT studies in bacterial pneumonia, such as Yu et al. (2024), which described uniform airway wall thickening and luminal narrowing in CAP.

The heterogeneity in Dh (mm) alterations across airway generations suggests that COVID-19 does not uniformly affect the bronchial tree but rather targets specific regions, possibly due to localized inflammatory or vascular injury (Ibrahim & Hassan, 2022; Karakasis et al., 2024). The preservation of Dh (mm) in certain distal branches, alongside significant proximal dilation may reflect compensatory mechanisms or differential susceptibility of airway segments to SARS-CoV-2 infection.

The hydraulic ratio (Xh), which reflects airflow efficiency, exhibited distinct spatial patterns across disease groups. Normal subjects displayed a steep proximal-to-distal gradient, consistent with physiological tapering of airways (Kuo et al., 2020). CAP patients, however, showed a flattened gradient, indicating a loss of structural differentiation. COVID-19 patients exhibited intermediate slopes, with HCVD preserving a more organized gradient than LCVD, suggesting a potential remodelling response that partially maintains airflow efficiency despite disease severity. Those findings are supported by many previous radiological and autopsy studies suggesting that SARS-CoV-2 primarily damages pulmonary vessels, causes airway wall swelling along the way and results in pulmonary interstitial and alveolar edema in the end (Ackermann et al., 2020; Xu et al., 2021). Notably, the left lung demonstrated greater heterogeneity in Xh patterns, particularly in mild COVID-19 cases, which may reflect asymmetrical disease progression or anatomical variations in airway susceptibility. These findings align with clinical observations of uneven lung involvement in COVID-19 (Gosangi et al., 2022; Haseli et al., 2020) and highlight the importance of regional assessments in understanding disease pathology.

Airway circularity further underscored the divergent remodelling patterns between COVID-19 and CAP. While CAP was associated with generalized increases in Cr, indicating more uniform luminal expansion, COVID-19 exhibited a heterogeneous response, with some airways showing increased circularity and others demonstrating significant reductions. This non-uniform remodelling suggests that COVID-19 induces localized geometric distortions, possibly due to asymmetric inflammation, thromboembolic events, or parenchymal traction as observed in many previous autopsy studies (Deshpande, 2020; Helmrich et al., 2020). The reduction in Cr in the left main bronchus and lower lobe branches aligns with prior observations in obstructive airway diseases, where geometric distortions increase resistance and impair ventilation (Maghsoudi-Ganjeh et al., 2021). In COVID-19, this may exacerbate hypoxemia by disrupting laminar flow and promoting turbulent airflow, particularly in severe (HCVD) cases with concomitant vascular pathology (Ramakrishnan et al., 2021).

The analysis of airway thickness revealed another layer of divergence between COVID-19 and CAP. While CAP was associated with mild diffuse airway thickening consistent with inflammatory infiltration, as previously observed in bacterial pneumonia structural imaging studies (Franquet, 2011), COVID-19 exhibited progressive airway thinning in severe cases, particularly affecting distal segments. Post-COVID follow-up CT studies have documented such evolving patterns of airway deformation—initial wall thickening followed by distal narrowing and architectural distortion (Caruso et al., 2021; Han et al., 2021). Coupled with our preservation of heterogeneity in morphometric metrics, this suggests a dual process involving generalized atrophy and focal thickening, potentially driven by endothelial injury and microthrombi, as demonstrated in histopathologic analyses of COVID-19 lungs (Ackermann et al., 2020) and supported by pulmonary diffusion abnormalities linked to vascular involvement (Frija-Masson et al., 2021). The paradoxical combination of diffuse thinning and localized thickenings may underlie the unique clinical course of COVID-19, where patients often present with severe hypoxemia despite relatively preserved lung mechanics (Swenson et al., 2021).

This study highlights the unique morphometric signature of COVID-19 airway remodelling, characterized by proximal dilation, heterogeneous geometric distortions, and diffuse wall thinning with focal thickenings. Such quantitative airway morphometry analysis may inform clinical decisions. Our quantitative airway analysis provides clinically actionable insights beyond descriptive characterization. For COVID-19 patients with hypoxemia, the observed proximal airway dilation and disrupted tapering patterns suggest that non-invasive respiratory support (NIV/CPAP or HFNO) could be optimized

by accounting for these structural changes when titrating flow and pressure parameters (Gorman et al., 2021; Weerakkody et al., 2022). The identification of distal ventilation-perfusion maldistribution through morphometric analysis may help select candidates most likely to benefit from awake prone positioning (Weatherald et al., 2022). In patients exhibiting CAP-like morphometric patterns characterized by diffuse airway narrowing, adjunctive airway-clearance techniques represent a rational therapeutic approach, though evidence for pharmacologic interventions remains limited (Belli et al., 2021). Importantly, our findings align with growing evidence that post-COVID airway remodelling, detectable through quantitative CT metrics, correlates with persistent pulmonary dysfunction (Colombi et al., 2023; Jia et al., 2022). This supports the potential role of generation-specific morphometry in long-term monitoring and risk stratification.

The findings in this study advance our understanding of COVID-19's pathophysiology and suggest that airway involvement may play a critical role in disease manifestations and outcomes. However, the mechanistic interpretations in this study remain hypotheses. While our morphometric data are consistent with prior pathological and imaging observations, direct histological or functional confirmation was beyond the scope of this study. Future research should focus on correlating these structural changes with functional assessments and exploring targeted interventions to mitigate airway remodelling in COVID-19 patients.

Several important limitations must be considered when interpreting the findings of this study. First, despite standardized reconstruction protocols, potential inter-scanner variability in the open-source dataset may introduce measurement bias, particularly for subtle morphometric changes. In addition, the smaller CAP cohort (n=38 vs. COVID-19 n=80) reduces statistical power for detecting modest between-group differences. Another limitation is the reliance on clinical CT scans with 2-mm slice thickness, which fundamentally constrains the accurate assessment of small airways beyond generation 6, potentially introducing measurement errors due to partial volume effects, particularly for distal airways approaching the scanner's resolution limit. The semi-automated airway reconstruction process, while necessary for quality control, may inadvertently normalize natural anatomical variations through manual editing and centreline generation algorithms that smooth out subtle pathological changes. In addition, the cross-sectional design cannot account for the temporal evolution of airway remodelling during different disease phases or potential recovery patterns, limiting our understanding of whether observed changes represent transient inflammation or permanent structural alterations.
While the study identifies distinct geometric patterns, the lack of correlation with pulmonary function tests or detailed symptom profiles makes it challenging to assess the clinical significance of these structural changes. The classification system may, therefore, oversimplify COVID-19's known clinical heterogeneity, and the potential influence of uncontrolled scanner parameters, including variations in kVp and mAs across subjects, introduces additional uncertainty in measurements. Furthermore, the absence of histopathological correlation leaves the biological mechanisms underlying the observed remodelling patterns somewhat speculative. These limitations highlight the need for future studies incorporating higher-resolution imaging, longitudinal assessments, and comprehensive clinical correlation to better understand the full spectrum of COVID-19's airway pathology and its functional consequences.

Conclusion

This comprehensive analysis of airway structural remodelling in COVID-19 pneumonia reveals distinct patterns of bronchial alteration that differ fundamentally from those observed in community-acquired pneumonia. Through systematic evaluation of Dh, Xh, Cr, and TA across multiple bronchial generations, this research has identified a characteristic signature of COVID-19 airway pathology characterized by proximal preservation with distal involvement, diffuse wall thinning with focal thickenings, and heterogeneous geometric remodelling. These divergent remodelling signatures suggest that COVID-19 impacts airway mechanics through mechanisms beyond those seen in bacterial pneumonia, potentially involving vascular injury, parenchymal traction, or differential inflammatory responses. The pronounced distal airway inefficiency and geometric deformation observed in COVID-19 may contribute to impaired ventilation, increased airway resistance, and the clinical features of silent hypoxemia. While the study has limitations related to resolution constraints and cross-sectional design, the consistent patterns observed across multiple airway parameters provide compelling evidence for COVID-19's unique bronchial involvement. Future research should focus on correlating these structural changes with longitudinal clinical outcomes, developing optimized imaging protocols for airway assessment, and investigating targeted interventions to prevent or mitigate COVID-19-related airway remodelling. The findings underscore the importance of considering airway pathology in both acute management and long-term follow-up of COVID-19 patients, and suggest that comprehensive respiratory evaluation in this population should include assessment of both proximal and distal airway function.

Funding

The study was not funded by external sources aside the author.

Data Availability

All data generated are represented in this manuscript.

Conflict of Interest

The authors declare no conflict of interest in this study

Author Contribution

The author confirms the sole responsibility for the conception of the study, presented results and manuscript preparation.

Declaration of Generative AI and AI-Assisted Technologies in the Writing Process

The author acknowledges that AI-assisted technologies were partially used in the preparation of this manuscript. Specifically, generative AI tools (ChatGPT and DeepSeek) were employed to support language refinement and grammar correction. All content was critically reviewed, edited, and approved by the author to ensure accuracy, originality, and alignment with academic standards. No AI tools were used to generate data, interpret results, or replace human intellectual contribution.

References

Ackermann, M., Verleden, S. E., Kuehnel, M., Haverich, A., Welte, T., Laenger, F., Vanstapel, A., Werlein, C., Stark, H., & Tzankov, A. (2020). Pulmonary vascular endothelialitis, thrombosis, and angiogenesis in Covid-19. *New England Journal of Medicine*, *383*(2), 120-128. https://doi.org/https://doi.org/10.1056/nejmoa2015432

Afshar, P., Heidarian, S., Enshaei, N., Naderkhani, F., Rafiee, M. J., Oikonomou, A., Fard, F. B., Samimi, K., Plataniotis, K. N., & Mohammadi, A. (2021). COVID-CT-MD, COVID-19 computed tomography scan dataset applicable in machine learning and deep learning. *Scientific Data*, *8*(1), 121. https://doi.org/10.1038/s41597-021-00900-3

Aghasafari, P., George, U., & Pidaparti, R. (2019). A review of inflammatory mechanism in airway diseases. *Inflammation Research*, *68*(1), 59-74. https://doi.org/https://doi.org/10.1007/s00011-018-1191-2

Bansal, M. (2020). Cardiovascular disease and COVID-19. *Diabetes & Metabolic Syndrome: Clinical Research & Reviews*, *14*(3), 247-250. https://doi.org/https://doi.org/10.1016/j.dsx.2020.03.013

Belli, S., Prince, I., Savio, G., Paracchini, E., Cattaneo, D., Bianchi, M., Masocco, F., Bellanti, M. T., & Balbi, B. (2021). Airway clearance techniques: the right choice for the right patient. *Frontiers in medicine*, *8*, 544826. https://doi.org/https://doi.org/10.3389/fmed.2021.544826

Caruso, D., Guido, G., Zerunian, M., Polidori, T., Lucertini, E., Pucciarelli, F., Polici, M., Rucci, C., Bracci, B., & Nicolai, M. (2021). Post-acute sequelae of COVID-19 pneumonia: six-month chest CT follow-up. *Radiology*, *301*(2), E396-E405. https://doi.org/https://doi.org/10.1148/radiol.2021210834

Choi, S., Hoffman, E. A., Wenzel, S. E., Castro, M., Fain, S., Jarjour, N., Schiebler, M. L., Chen, K., & Lin, C. L. (2017). Quantitative computed tomographic imaging-based clustering differentiates asthmatic subgroups with distinctive clinical phenotypes. *J Allergy Clin Immunol*, *140*(3), 690-700.e698. https://doi.org/10.1016/j.jaci.2016.11.053

Choi, S., Hoffman, E. A., Wenzel, S. E., Castro, M., Fain, S. B., Jarjour, N. N., Schiebler, M. L., Chen, K., & Lin, C. L. (2015). Quantitative assessment of multiscale structural and functional alterations in asthmatic populations. *J Appl Physiol (1985)*, *118*(10), 1286-1298. https://doi.org/10.1152/japplphysiol.01094.2014

Colombi, D., Petrini, M., Risoli, C., Mangia, A., Milanese, G., Silva, M., Franco, C., Sverzellati, N., & Michieletti, E. (2023). Quantitative CT at Follow-Up of COVID-19 Pneumonia: Relationship with Pulmonary Function Tests. *Diagnostics*, *13*(21), 3328. https://doi.org/https://doi.org/10.3390/diagnostics13213328

Cozzi, D., Cavigli, E., Moroni, C., Smorchkova, O., Zantonelli, G., Pradella, S., & Miele, V. (2021). Ground-glass opacity (GGO): a review of the differential diagnosis in the era of COVID-19. *Japanese journal of radiology*, *39*(8), 721-732. https://doi.org/https://doi.org/10.1007/s11604-021-01120-w

D'Arena, G., Penna, A. L., Crocamo, A., Sguazzo, F., Viceconti, R., Barlotti, V., & Gambardella, M. (2021). Heterogeneity of clinical and radiological findings of COVID-19. *Postgraduate Medical Journal*, *97*(1146), 268-269. https://doi.org/https://doi.org/10.1136/postgradmedj-2020-137901

Deshpande, C. (2020). Thromboembolic findings in COVID-19 autopsies: pulmonary thrombosis or embolism? *Annals of internal medicine*, *173*(5), 394-395. https://doi.org/https://doi.org/10.7326/m20-3255

Dhochak, N., Singhal, T., Kabra, S., & Lodha, R. (2020). Pathophysiology of COVID-19: why children fare better than adults? *The Indian Journal of Pediatrics*, *87*(7), 537-546. https://doi.org/https://doi.org/10.1007/s12098-020-03322-y

Dournes, G. (2025). Quantitative CT Imaging of Chronic Airway Diseases. In *Medical Radiology*. Springer, Berlin, Heidelberg. https://doi.org/https://doi.org/10.1007/174_2025_606

Eskandari, M., Kuschner, W. G., & Kuhl, E. (2015). Patient-Specific Airway Wall Remodeling in Chronic Lung Disease. *Ann Biomed Eng*, *43*(10), 2538-2551. https://doi.org/10.1007/s10439-015-1306-7

Feragen, A., Petersen, J., Owen, M., Lo, P., Thomsen, L. H., Wille, M. M. W., Dirksen, A., & Bruijne, M. d. (2015). Geodesic Atlas-Based Labeling of Anatomical Trees: Application and Evaluation on Airways Extracted From CT. *IEEE Transactions on Medical Imaging*, *34*(6), 1212-1226. https://doi.org/10.1109/TMI.2014.2380991

Franquet, T. (2011). Imaging of pulmonary viral pneumonia. *Radiology*, *260*(1), 18-39. https://doi.org/https://doi.org/10.1148/radiol.11092149

Frija-Masson, J., Bancal, C., Plantier, L., Benzaquen, H., Mangin, L., Penaud, D., Arnoult, F., Flamant, M., & d'Ortho, M.-P. (2021). Alteration of diffusion capacity after SARS-CoV-2 infection: a pathophysiological approach. *Frontiers in Physiology*, *12*, 624062. https://doi.org/https://doi.org/10.3389/fphys.2021.624062

Gattinoni, L., Chiumello, D., Caironi, P., Busana, M., Romitti, F., Brazzi, L., & Camporota, L. (2020). COVID-19 pneumonia: different respiratory treatments for different phenotypes? *Intensive Care Medicine*, *46*(6), 1099-1102. https://doi.org/10.1007/s00134-020-06033-2

Goodwill, A. G., Dick, G. M., Kiel, A. M., & Tune, J. D. (2017). Regulation of Coronary Blood Flow. *Compr Physiol*, *7*(2), 321-382. https://doi.org/10.1002/cphy.c160016

Gorman, E., Connolly, B., Couper, K., Perkins, G. D., & McAuley, D. F. (2021). Non-invasive respiratory support strategies in COVID-19. *The Lancet Respiratory Medicine*, *9*(6), 553-556. https://doi.org/https://doi.org/10.1016/s2213-2600(21)00168-5

Gosangi, B., Rubinowitz, A. N., Irugu, D., Gange, C., Bader, A., & Cortopassi, I. (2022). COVID-19 ARDS: a review of imaging features and overview of mechanical ventilation and its complications. *Emergency radiology*, *29*(1), 23-34. https://doi.org/https://doi.org/10.1007/s10140-021-01976-5

Han, X., Fan, Y., Alwalid, O., Li, N., Jia, X., Yuan, M., Li, Y., Cao, Y., Gu, J., & Wu, H. (2021). Six-month follow-up chest CT findings after severe COVID-19 pneumonia. *Radiology*, *299*(1), E177-E186. https://doi.org/https://doi.org/10.1148/radiol.2021203153

Haseli, S., Khalili, N., Bakhshayeshkaram, M., Sanei Taheri, M., & Moharramzad, Y. (2020). Lobar Distribution of COVID-19 Pneumonia Based on Chest Computed Tomography Findings; A Retrospective Study. *Arch Acad Emerg Med*, *8*(1), e55.

Helmrich, E., Decker, L., Adolphi, N., & Makino, Y. (2020). Postmortem CT lung findings in decedents with Covid-19: a review of 14 decedents and potential triage implications. *Forensic Imaging*, *23*, 200419. https://doi.org/https://doi.org/10.1016/j.fri.2020.200419

Ibrahim, G., & Hassan, A. (2022). CT-based Analysis of Vascular Tree Abnormalities in Different Phenotypes of COVID-19 Pneumonia. *Int. J. Adv. Sci. Eng. Inf. Technol.*, *12*(3), 1215–1221. https://doi.org/https://doi.org/10.18517/ijaseit.12.3.12579

Jia, X., Han, X., Cao, Y., Fan, Y., Yuan, M., Li, Y., Gu, J., Zheng, Y., Wang, L., & Qu, Y. (2022). Quantitative inspiratory–expiratory chest CT findings in COVID-19 survivors at the 6-month follow-up. *Scientific Reports*, *12*(1), 7402. https://doi.org/https://doi.org/10.1038/s41598-022-11237-1

Karakasis, P., Nasoufidou, A., Sagris, M., Fragakis, N., & Tsioufis, K. (2024). Vascular Alterations Following COVID-19 Infection: A Comprehensive Literature Review. *Life (Basel)*, *14*(5). https://doi.org/10.3390/life14050545

Kuo, W., Perez-Rovira, A., Tiddens, H., & de Bruijne, M. (2020). Airway tapering: an objective image biomarker for bronchiectasis. *Eur Radiol*, *30*(5), 2703-2711. https://doi.org/10.1007/s00330-019-06606-w

Long, M. E., Mallampalli, R. K., & Horowitz, J. C. (2022). Pathogenesis of pneumonia and acute lung injury. *Clinical Science*, *136*(10), 747-769. https://doi.org/https://doi.org/10.1042/cs20210879

Louis, D. W., Saad, M., Vijayakumar, S., Ilyas, S., Kokkirala, A., & Aronow, H. D. (2023). The cardiovascular manifestations of COVID-19. *Heart Failure Clinics*, *19*(2), 153. https://doi.org/https://doi.org/10.1016/j.hfc.2022.08.001

Maghsoudi-Ganjeh, M., Sattari, S., & Eskandari, M. (2021). Mechanical behavior of the airway wall in respiratory disease. *Current Opinion in Physiology*, *22*, 100445. https://doi.org/https://doi.org/10.1016/j.cophys.2021.05.008

Mahdavi, M. M. B., Arabfard, M., Rafati, M., & Ghanei, M. (2023). A computer-based analysis for identification and quantification of small airway disease in lung computed tomography images: a comprehensive review for radiologists. *Journal of Thoracic Imaging*, *38*(1), W1-W18. https://doi.org/https://doi.org/10.1097/rti.0000000000000683

Meyerholz, D. K., & Reznikov, L. R. (2022). Influence of SARS-CoV-2 on airway mucus production: A review and

proposed model. *Vet Pathol*, *59*(4), 578-585. https://doi.org/10.1177/03009858211058837

Ortiz-Puerta, D., Diaz, O., Retamal, J., & Hurtado, D. E. (2023). Morphometric analysis of airways in pre-COPD and mild COPD lungs using continuous surface representations of the bronchial lumen. *Frontiers in Bioengineering and Biotechnology*, *11*, 1271760. https://doi.org/https://doi.org/10.3389/fbioe.2023.1271760

Park, H. J., Lee, S. M., Choe, J., Lee, S. M., Kim, N., Lee, J. S., Oh, Y. M., & Seo, J. B. (2019). Prediction of Treatment Response in Patients with Chronic Obstructive Pulmonary Disease by Determination of Airway Dimensions with Baseline Computed Tomography. *Korean J Radiol*, *20*(2), 304-312. https://doi.org/10.3348/kjr.2018.0204

Patil, S., Tandel, N., Kasture, L., & Gondhali, G. (2023). Radiological patterns integration with duration of illness in COVID-19 pneumonia as 'evolved'and 'evolving'radiological phenotypes: a single center experience. *Journal of Medicine*, *24*(2), 71-81. https://doi.org/https://doi.org/10.3329/jom.v24i2.67268

Ramakrishnan, K., Kumaran, M., Townsend, R., & Weir, M. (2021). Clinical advances in the evaluation of patients with excessive central airway collapse: a narrative review. *Journal of Visualized Surgery*, *8*. https://doi.org/https://doi.org/10.21037/jovs-21-6

Roig-Marín, N. (2024). Ground-glass nodules in the lungs of COVID-19 patients. In *Management, Body Systems, and Case Studies in COVID-19* (pp. 237-244). Elsevier.

Shi, H., Han, X., Jiang, N., Cao, Y., Alwalid, O., Gu, J., Fan, Y., & Zheng, C. (2020). Radiological findings from 81 patients with COVID-19 pneumonia in Wuhan, China: a descriptive study. *The Lancet infectious diseases*, *20*(4), 425-434. https://doi.org/https://doi.org/10.1016/s1473-3099(20)30086-4

Swenson, K. E., Ruoss, S. J., & Swenson, E. R. (2021). The pathophysiology and dangers of silent hypoxemia in COVID-19 lung injury. *Annals of the American Thoracic Society*, *18*(7), 1098-1105. https://doi.org/https://doi.org/10.1513/annalsats.202011-1376cme

Weatherald, J., Parhar, K. K. S., Al Duhailib, Z., Chu, D. K., Granholm, A., Solverson, K., Lewis, K., Møller, M. H., Alshahrani, M., & Belley-Cote, E. (2022). Efficacy of awake prone positioning in patients with covid-19 related hypoxemic respiratory failure: systematic review and meta-analysis of randomized trials. *Bmj*, *379*. https://doi.org/https://doi.org/10.1136/bmj-2022-071966

Weerakkody, S., Arina, P., Glenister, J., Cottrell, S., Boscaini-Gilroy, G., Singer, M., & Montgomery, H. E. (2022). Non-invasive respiratory support in the management of acute COVID-19 pneumonia: considerations for clinical practice and priorities for research. *The Lancet Respiratory Medicine*, *10*(2), 199-213. https://doi.org/https://doi.org/10.1016/S2213-2600(21)00414-8

Xu, J., Liang, Z., Jian, W., Li, J., Tang, G., Mo, X., Zhang, D., Zheng, J., Qian, Y., Liu, J., & Li, S. (2021). Changes of quantitative CT-based airway wall dimensions in patients with COVID-19 during early recovery. *J Thorac Dis*, *13*(3), 1517-1530. https://doi.org/10.21037/jtd-20-2790

Yu, W., Shi, Y., Zheng, Q., Chen, J., Zhang, X., Chen, A., Yu, Z., Zhou, W., Lin, L., Zheng, L., Ye, H., & Li, Y. (2024). Comparison between community-acquired pneumonia and post-obstructive pneumonia associated with endobronchial tumors. *BMC Pulm Med*, *24*(1), 589. https://doi.org/10.1186/s12890-024-03409-8

Zaremba, S., Miller, A. J., Ovrom, E. A., Senefeld, J. W., Wiggins, C. C., Dominelli, P. B., Ganesh, R., Hurt, R. T., Bartholmai, B. J., Welch, B. T., Ripoll, J. G., Joyner, M. J., & Ramsook, A. H. (2024). Increased luminal area of large conducting airways in patients with COVID-19 and post-acute sequelae of COVID-19: a retrospective case-control study. *J Appl Physiol (1985)*, *137*(5), 1168-1174. https://doi.org/10.1152/japplphysiol.00573.2024